



**Providing Choice & Value**  
Generic CT and MRI Contrast Agents

**FRESENIUS  
KABI**

**CONTACT REP**

**AJNR**

## **Intraspinal Paragonimiasis in Children: MRI Findings and Suggestions for Pathogenesis**

Y. Qin, J. Cai, W. Ji, X. Chen, L. Tian, S. Jun, L. Wang and X. He

*AJNR Am J Neuroradiol* 2019, 40 (12) 2166-2171

doi: <https://doi.org/10.3174/ajnr.A6296>

<http://www.ajnr.org/content/40/12/2166>

This information is current as  
of July 28, 2025.

# Intraspinal Paragonimiasis in Children: MRI Findings and Suggestions for Pathogenesis

Y. Qin, J. Cai, W. Ji, X. Chen, L. Tian, S. Jun, L. Wang, and X. He

## ABSTRACT

**BACKGROUND AND PURPOSE:** Intraspinal paragonimiasis is a rare entity for which imaging findings have seldom been described. The present study investigated the MR imaging features of spinal paragonimiasis, thus providing diagnostic imaging evidence and exploring the possible pathogenesis of intraspinal paragonimiasis.

**MATERIALS AND METHODS:** The clinical and imaging findings of spinal paragonimiasis in 6 children were analyzed retrospectively. Spinal MR imaging was performed in all patients, 5 of whom also underwent enhanced MR imaging. The diagnosis was confirmed by enzyme-linked immunosorbent assay in all cases and postoperative pathology in 4 cases.

**RESULTS:** All cases manifested as fusiform-shaped or beanlike masses in the extradural space in the thoracic spine. The extradural masses were connected with pleural lesions through the intervertebral foramen. The plain MR imaging scan showed mixed signals with predominant isointensity on T1WI and hyperintensity on T2WI, among which 5 (5/6) masses presented as patchy hemorrhage with hyperintensity on T1WI. On enhanced scans, all masses (5/5) showed heterogeneous marked enhancement, with thickening and enhancement in the adjacent spinal meninges (5/5). Various degrees of spinal cord compression and edema were found in 5 cases (5/6).

**CONCLUSIONS:** MR imaging is sensitive for detecting and characterizing spinal paragonimiasis. The MR imaging features of intraspinal granulomas included localization to the extradural space and thoracic segment, connections between intraspinal lesions and pleural lesions through the intervertebral foramen, and hemorrhagic foci within the mass. These findings support an intraspinal mode of paragonimiasis pathogenesis: The *Paragonimus* larvae migrate from the chest into the extradural space through the intervertebral foramen.

Paragonimiasis is an infestation caused by a lung fluke of the genus *Paragonimus*.<sup>1</sup> Human infection is usually caused by eating raw or undercooked crayfish that harbor these parasites or drinking infested fresh water. The metacercariae of the *Paragonimus* excyst in the small intestine penetrate through the intestinal wall into the peritoneal cavity, then migrate through the diaphragm to the pleural space and into the lungs, and finally become adult organisms. For some species, the lung flukes cannot develop into adults in humans, and the larvae can migrate into other sites from the lung or pleural spaces.<sup>1</sup> The CNS is the most common site of extrapulmonary paragonimiasis.<sup>2</sup> Intracranial paragonimiasis has been comprehensively reported, and some imaging features have been summarized and regarded as

important diagnostic evidence.<sup>3,4</sup> However, only a few isolated cases with occurrence in the spinal canal have been reported.<sup>5-8</sup>

In a review of the literature, most of these cases were reported in the 1950s and 1960s, without any description of CT and/or MR imaging findings<sup>5-7</sup> because no modern imaging device was available at that time. Because neuroimaging, especially MR imaging, can accurately localize and comprehensively demonstrate lesions, this technique plays an important role in the diagnosis and differential diagnosis of intraspinal diseases<sup>9,10</sup>; it is crucial to summarize and analyze the imaging features of intraspinal paragonimiasis. Here, we report 6 cases of intraspinal extradural paragonimiasis, with a detailed description of the clinical and MR imaging findings. Then, we discuss the possible pathogenesis of spinal paragonimiasis based on imaging evidence.

## MATERIALS AND METHODS

### General Patient Information

This study was approved by the Research Ethics Committee of the Children's Hospital of Chongqing Medical University.

Received June 8, 2019; accepted after revision September 3.

From the Departments of Radiology (Y.Q., J.C., L.T., S.J., L.W., X.H.), Outpatient Surgery (X.C.), and Neurosurgery (W.J.), Children's Hospital of Chongqing Medical University, Chongqing, China.

Please address correspondence to Jinhua Cai, MD, Children's Hospital of Chongqing Medical University, 136 Zhongshan 2nd Rd, Yuzhong District, Chongqing, China 400014; e-mail: cai\_jinhua@126.com

<http://dx.doi.org/10.3174/ajnr.A6296>

Informed consent was obtained from all patients included in the study. Six patients with spinal paragonimiasis (5 boys and 1 girl; ranging from 5 to 12 years of age, with a mean of 8.2 years) were selected from 83 patients with CNS involvement in a total of 723 patients with paragonimiasis diagnosed in our hospital during the past 10 years (January 2008 to January 2018). All cases were from southwest China, the epidemic area of lung flukes, including Chongqing ( $n=4$ ), Sichuan ( $n=1$ ), and Guizhou ( $n=1$ ) provinces. The most common chief symptom of these patients was weak lower limbs and back pain. The diagnosis was confirmed by an enzyme-linked immunosorbent assay for *Paragonimus*-specific antibody (immunoglobulin G) in serum (6/6) and postoperative pathology (4/6).

### **Clinical Symptoms and History**

The main clinical manifestations were lower extremity weakness ( $n=4$ ) and thoracolumbar pain ( $n=2$ ), of which 1 case was complicated by sensory disorders. All 6 patients were complicated by pleural lesions, and among these patients, 2 patients were complicated by pulmonary paragonimiasis. Regarding their life history, 3 patients reported a history of eating raw or undercooked crabs, one reported a history of drinking fresh water, and 2 patients had an unknown history of infection.

### **Laboratory Examination**

The blood examinations of the 6 patients with spinal paragonimiasis all showed eosinophil counts that were increased to varying degrees, ranging from 8% to 47%. Lumbar puncture for CSF analysis was performed in 4 patients. The CSF appeared colorless and transparent in all patients. In 1 patient, the CSF pressure increased to 215 mm H<sub>2</sub>O, with the eosinophil counts increasing to 19%, while in the other patients, the CSF pressure (80–180 mm H<sub>2</sub>O) and eosinophil counts were normal. Enzyme-linked immunosorbent assays in serum were performed, and the results were positive for *Paragonimus* antibody in all cases.

### **Therapy and Prognosis**

Two patients were treated with oral administration of praziquantel alone at a dose of 25 mg/kg administered 3 times per day for 3 consecutive days, followed by an intermission of 4 days, after which this course was repeated for 9 weeks. Subsequently, the clinical manifestations disappeared, and the physical examination revealed no abnormalities. The other 4 patients underwent surgical removal of the masses under general anesthesia, and then praziquantel was orally administered. The dosage and duration of the treatment were the same as for those receiving oral administration alone. No dysfunction of movement or sensation was found in the 3–6 months of follow-up.

### **MR Imaging Examination**

All 6 patients underwent plain MR imaging, and 5 patients underwent enhanced imaging. The shortest length of time from onset to the imaging examination was 2 days, while the longest was 30 days, with a mean duration of 7 days. The follow-up MR imaging was performed 1 week after surgical removal or after 10 courses of medical treatment. All MR imaging examinations were performed using a 1.5T MR imaging scanner (Signa Excite HD; GE Healthcare, Milwaukee, Wisconsin) or a 3T MR imaging

scanner (Achieva; Philips Healthcare, Best, the Netherlands) with a spine coil. The scan sequences included sagittal and axial spin-echo T1WI and T2WI. The scan parameters were as follows—T1WI: TR of 400–460 ms, TE of 8–12 ms; T2WI: TR of 3000–6000 ms, TE of 90–120 ms; thickness of 3–6 mm, distance of 2–3 mm, matrix of  $266 \times 266$ , and 2–4 excitations. A contrast-enhanced T1WI scan was obtained after intravenous injection of GD-DTPA at a dose of 0.2 mL/kg.

## **RESULTS**

### **Lesion Location**

Five lesions were located within the thoracic spine (Figs 1A, -B), while 1 lesion was located in the junction of thoracolumbar segments (Figs 2A, -B). In the axial direction of the spine, all 6 lesions involved the intraspinal extradural space; additionally, the 6 lesions were all connected with the pleural lesions through the intervertebral foramen (Figs 1C, -D and 2C, -D).

### **Lesion Morphology**

The sagittal view showed fusiform-shaped (5/6) or bean-shaped (1/6) masses in the extradural space, and the longitudinal diameter passed 4–10 vertebral bodies, with a length ranging from 5.9 to 16.7 cm. The axial view showed that the granulomatous lesions of the 6 patients were all connected to pleural lesions (including pleural thickening in 6, pleural effusion in 4, and subpleural nodules in 4) through the intervertebral foramen, similar to the dumbbell-like sign (Figs 1C, -D and 2C, -D).

### **MR Imaging Signal**

The plain MR imaging scan of the 6 granulomatous lesions showed mixed signals with predominant isointensity on T1WI (Figs 1A, -C and 2A, -C) and hyperintensity on T2WI (Figs 1B, -D and 2B, -D), of which 5 fusiform-shaped lesions presented with multiple patchlike or irregular hemorrhagic foci with hyperintensity on T1WI within the masses (Figs 1A, -C and 2A, -C). The 5 patients undergoing the enhanced MR image showed heterogeneous and marked enhancement in the granulomatous masses (Figs 1E, -F and 2E, -F). The lesions in the intervertebral foramen and the pleura showed an enhancement pattern that was similar to that in the intraspinal lesions (Figs 1F and 2F). Furthermore, there was enhancement in the adjacent spinal meninges (Figs 1E and 2E).

### **Spinal Cord**

In 5 of the 6 patients, the corresponding segment of the spinal cord exhibited various degrees of compression and edema, which was visible as hyperintensity on T2WI (Fig 1B, -D).

### **Combined Lesions**

All 6 spinal paragonimiasis cases were complicated by pleural lesions, including 6 cases of pleural thickening, 4 cases with a small amount of pleural effusion, and 4 cases of subpleural nodules. The chest CT of 2 patients showed pulmonary nodules and stripe-shaped small cavity lesions. However, no clinical or imaging evidence of cerebral paragonimiasis was found in the 6 spinal paragonimiasis cases.

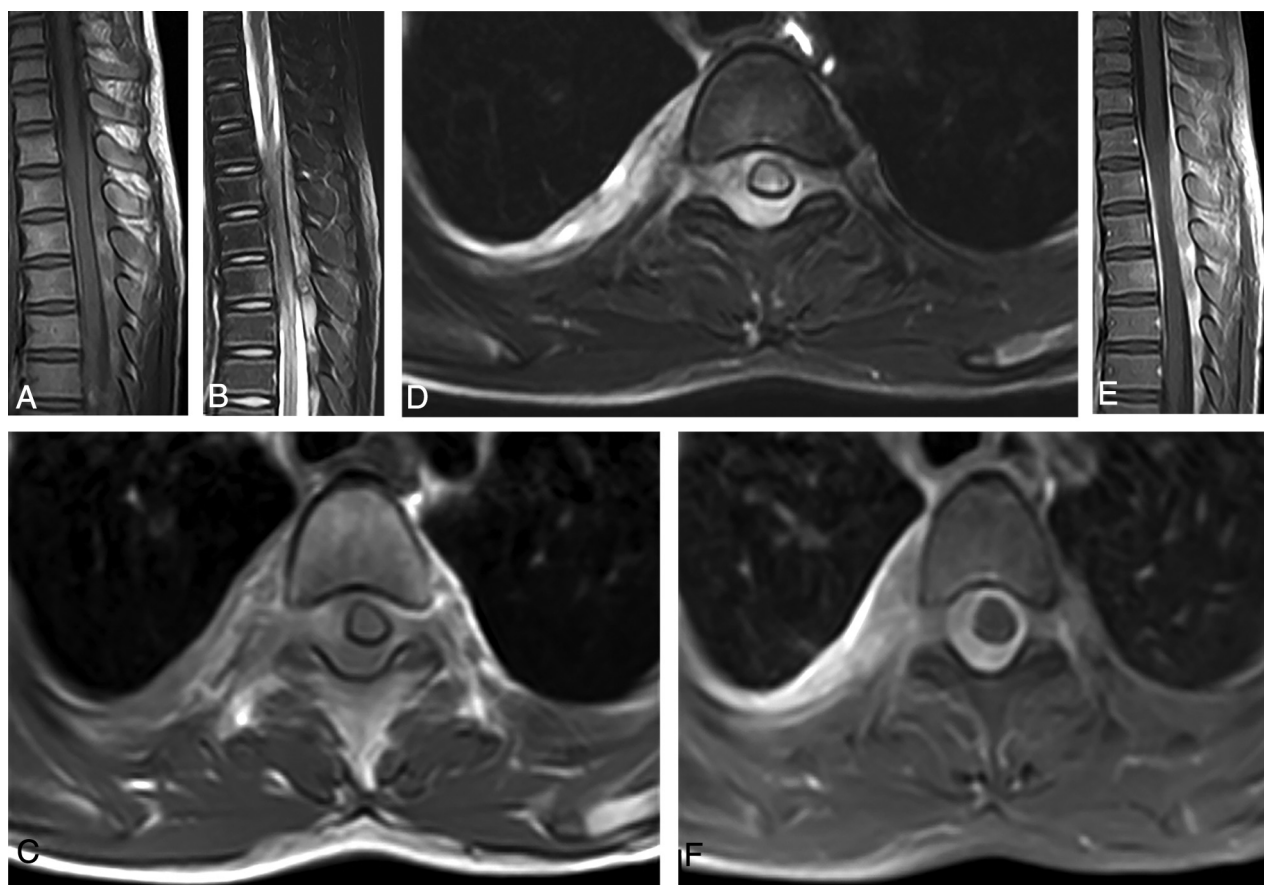


**FIG 1.** MR imaging of intraspinal paragonimiasis in a 6-year-old patient. Sagittal TIWI (A) and T2WI (B) show a longitudinal fusiform-shaped mass located in the intraspinal extradural space parallel to the level of T2–T11, with predominant isointensity on TIWI and hyperintensity on T2WI, and there are multiple patchlike hemorrhagic areas with hyperintensity on TIWI and hypointensity on T2WI within the mass. Axial TIWI (C) and T2WI (D) show that the mass is located in the extradural space and extends to the right intervertebral foramen, connecting to the irregularly thickened pleural lesions on the right, accompanied by a small amount of pleural effusion. The compressed spinal cord moves slightly to the left front, and there is edema with hyperintensity on T2WI. The sagittal (E) and axial (F) views of the contrast-enhanced images indicate that the mass is obviously enhanced, and there are scattered nonenhancement areas within it. Additionally, the adjacent spinal meninges show obvious enhancement.

### Follow-Up MR Imaging

After treatment with oral medication or surgical removal, the follow-up MR imaging showed that the masses were reduced or had disappeared. The spinal cord compression was completely relieved, and the edema with hyperintensity on T2WI had disappeared.

### Pathologic Findings

The macroscopic observation of the pathologic specimens showed grayish-white tissue with a soft and loose texture, and hemorrhage and necrosis were found on the cut surface. The microscopic observation showed tunnels within the granulomas, and a large number of eosinophils and lymphocytes invaded the granulomatous tissue around the tunnel. Furthermore, a large number of erythrocytes were found in some regions.

### DISCUSSION

*Paragonimus* infection can invade various parenchymal organs and tissues, including the lungs, pleura, brain, liver, and sub-

cutaneous tissue.<sup>3,11–17</sup> The infection involving the CNS is rare and constitutes approximately 0.8%–31.0% of all active paragonimiasis.<sup>3</sup> Spinal involvement is even more uncommonly encountered, with the occurrence ranging from 2% to 10% among CNS paragonimiasis.<sup>5</sup> In our series, only 6 cases of spinal involvement occurred among 83 patients with CNS paragonimiasis (7.2%, 6/83), which is similar to that in previous reports.

The pathogenesis of the formation of spinal paragonimiasis is still uncertain.<sup>1,5–8,18</sup> Several theories have been proposed in previous reports. The first is that the *Paragonimus* larvae may directly migrate from the lung and/or pleura to the spinal canal through the paravertebral soft tissue.<sup>5</sup> A second theory was suggested by Diaconita and Nagy<sup>18</sup> in 1957, which stated that paragonimiasis involvement in the spinal canal could result from hematogenous extension. Another theory was that the infection of the spinal canal was caused by the direct downward movement of cerebral paragonimiasis.<sup>5</sup> The above theories regarding the spinal involvement of paragonimiasis are conflicting, and none of these notions have been confirmed by any clear imaging or other evidence. In this study, the imaging findings of the 6 extradural

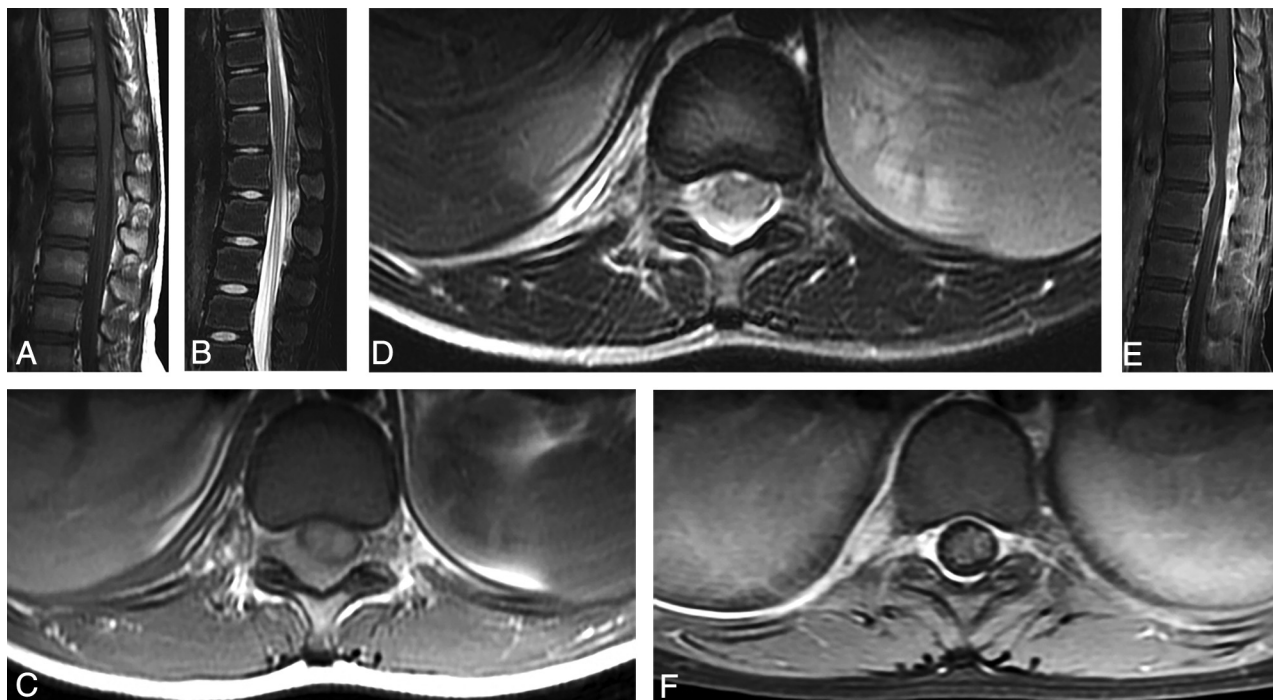


**FIG 2.** MR imaging of intraspinal paragonimiasis in a 12-year-old patient. Sagittal TIWI (A) and T2WI (B) show a fusiform-shaped mass located in the intraspinal extradural space at the junction of the thoracolumbar spine (T10–L2). The mass shows a heterogeneous signal with multiple patchy hemorrhage foci. Axial TIWI (C) and T2WI (D) show that the mass is located in the extradural space and connects with the irregular pleural lesions through the right intervertebral foramen. The spinal cord is compressed, but there is no edema. The sagittal view of the contrast imaging (E) shows a heterogeneous and significant enhancement in the extradural masses, and the axial view (F) also shows significant enhancement in the intervertebral foramen and pleural lesions. Meanwhile, the adjacent spinal meninges show thickening and enhancement.

spinal paragonimiasis cases provided strong evidence for a mechanism of pathogenesis in which the lung flukes directly invade the spinal canal from the pleural lesions through the intervertebral foramen. First, all the intraspinal granulomatous masses in this series occurred in thoracic segments, also consistent with the report from Moon et al<sup>5</sup> showing that thoracic spines were involved in all 8 patients with spinal paragonimiasis examined in that study. Second, all the lesions located in the extradural space were connected to the pleural lesions through the intervertebral foramen. This physical connection indicated that the intraspinal extradural lesions were from the adjacent pleural (or pulmonary) lesions. Third, no imaging evidence of either cervical paragonimiasis or cerebral paragonimiasis was found in this group of patients; therefore, the possibility that extradural spinal paragonimiasis was caused by the downward movement of cerebral paragonimiasis could be excluded. In addition, no imaging or laboratory data in our cases supported the theory of hematogenous extension.

On the basis of the mode of invasion of paragonimiasis from the pleura to the spinal canal, the extradural space could be inevitably invaded. This has been confirmed in our cases and in most previously reported cases.<sup>5–7</sup> However, in the previous reports, there were a few cases complicated by intradural or/and spinal cord involvement except for extradural invasion. There has been no reasonable explanation for this phenomenon. We speculate that the intradural or/and spinal cord lesions could be a result of migration from the extradural space. Because the *Paragonimus* larvae habitually migrate, they can penetrate the intestinal wall,

pleura, and meninges. In this mode, they can also penetrate the dura mater and the soft spinal membrane, resulting in intraspinal or/and spinal lesion formation. Whether the intradural or/and spinal cord lesions occur could be determined by the progression of the disease. In our series, the lesions in all cases were limited in the extradural space. This could be attributed to the early detection achieved via the application of modern imaging technology.

As with cerebral paragonimiasis, hemorrhage is also considered a very important imaging feature in the diagnosis of spinal paragonimiasis. In this group of patients, 83.3% (5/6) had hemorrhage, which showed patchy hyperintensity on T1WI and hypointensity on T2WI. The hemorrhagic tendency of paragonimiasis could be attributed to the biologic behavior of the parasite.<sup>19–21</sup> When the worm entered the epidural space through the intervertebral foramen, it formed granulomatous lesions; additionally, the migration of worms can cause hyperemia, vasculitis, and broken capillaries, resulting in hemorrhage.<sup>1,19</sup> In addition, hemorrhage is more likely to occur in children because their blood vessels are more vulnerable than those of adults. In this study, the granuloma of 1 patient did not show hemorrhage with obvious hyperintensity on T1WI, which may be due to the small size of the granulomatous lesion or the different maturity grades of the granuloma.<sup>20,22</sup>

The laboratory tests, including the eosinophil counts, the dot-immunogold filtration assay, and enzyme-linked immunosorbent assay, have high specificity and sensitivity to detect paragonimiasis.<sup>1,23</sup> These methods, however, are unable to locate or characterize the lesions. Although myelography was also used for the

detection of spinal paragonimiasis lesions by Moon et al,<sup>5</sup> it is an invasive method and the imaging results are nonspecific, with a low positive rate; thus, this technique is now rarely used. Compared with myelography, MR imaging has the advantage of multiplane imaging and excellent contrast of the soft tissue, which is especially suitable for displaying spinal lesions. In this study, MR imaging not only clearly revealed the location, range, and size of lesions but also found the signal features of the hemorrhage in spinal paragonimiasis, as well as its relationship with the spinal cord, thus providing useful information for the early diagnosis of spinal paragonimiasis and surgical treatment.

Because of some similarities in their imaging manifestations, extradural spinal paragonimiasis needs to be differentiated from the following diseases:

1) Neurogenic tumors: because the intraspinal soft-tissue masses of spinal paragonimiasis are connected to the paravertebral and pleural lesions through the intervertebral foramen, the lesions appear to be distributed along the spinal nerves, similar to the dumbbell-like sign, and they are easily misdiagnosed as neurogenic tumors.<sup>24</sup> However, they can be differentiated on the basis of the following features: First, in most cases, the dumbbell-like mass formed by neurogenic tumors has a well-defined boundary, with an enlarged intervertebral foramen and even bone absorption and destruction, while spinal paragonimiasis presents with the exact opposite features. Second, the mass of spinal paragonimiasis is closely related to the pleura with thickening, pleural nodularity, and enhancement. However, in neurogenic tumors, only a few cases showed adjacent slightly pleural responses. Third, paragonimiasis has a tendency to produce hemorrhage, while neurogenic tumors have no such tendency.

2) Tuberculoma or bacterial abscess: tuberculoma is often encountered in the intraspinal extradural space. It shares a similar lesion location and enhancement patterns with paragonimiasis and is also frequently accompanied by pleural and intrapulmonary lesions. However, hemorrhage with hyperintensity on T1WI is seldom observed in intraspinal extradural tuberculoma. In addition, intraspinal tuberculomas are usually accompanied by vertebral or intracranial invasion.<sup>9</sup> Bacterial abscess is another infectious disease that can form a mass in the intraspinal extradural space. For this disease, enhanced MR imaging usually shows a ring-shaped enhancement, which is different from the substantial enhancement pattern of paragonimiasis granuloma.

3) Intraspinal hematoma: because hemorrhage in granulomas is common in spinal paragonimiasis, it must be differentiated from intraspinal hematoma. In the early stages, intraspinal hematoma usually presents with uniform hyperintensity on T1WI and does not extend to the subpleural space through the intervertebral foramen. Moreover, intraspinal hematoma could change the signal features on follow-up MR imaging.<sup>25</sup>

4) Lymphomas: most extradural lymphomas usually present with uniform signals on plain and enhanced scans<sup>26</sup>; however, intraspinal paragonimiasis granulomas often present with heterogeneous signals because of internal hemorrhage.

5) Angiomyolipomas: this tumor occasionally occurs in the epidural space and needs to be considered in the differential diagnosis.<sup>27</sup> The fat composition in angiomyolipomas can be easily detected by MR imaging; this feature could be helpful in

differentiating it from paragonimiasis. In addition to the differences in imaging features, the *Paragonimus* endemic areas (especially in East Asia), the increased eosinophil counts in laboratory examinations, and the antibody test by enzyme-linked immunosorbent assay are also strong evidence for the diagnosis of spinal paragonimiasis and the exclusion of all the aforementioned diseases.

## CONCLUSIONS

Spinal paragonimiasis is a very rare entity and can be sensitively detected by MR imaging. On MR imaging, the intraspinal granulomas often present as a longitudinal fusiform-shaped or beanlike mass located in the thoracic segment and the extradural space and connect to pleural lesions through the intervertebral foramen. Hemorrhagic foci within the mass are a significant imaging feature, which is consistent with the imaging features of cerebral paragonimiasis. These MR imaging findings provide strong evidence for the following mode of pathogenesis for extradural spinal paragonimiasis: The *Paragonimus* larvae migrate from the primary chest lesions into the intraspinal extradural space through the intervertebral foramen instead of by hematogenous extension or by downward movement of cerebral paragonimiasis.

## REFERENCES

- Chai JY. **Paragonimiasis.** *Handb Clin Neurol* 2013;114:283–96 [CrossRef Medline](#)
- Nawa Y. **Re-emergence of paragonimiasis.** *Intern Med* 2000;39:353–54 [CrossRef Medline](#)
- Chen J, Chen Z, Lin J, et al. **Cerebral paragonimiasis: a retrospective analysis of 89 cases.** *Clin Neurol Neurosurg* 2013;115:546–51 [CrossRef Medline](#)
- Xia Y, Chen J, Ju Y, et al. **Characteristic CT and MR imaging findings of cerebral paragonimiasis.** *J Neuroradiol* 2016;43:200–06 [CrossRef Medline](#)
- Moon TJ, Yoon BY, Hahn YS. **Spinal paragonimiasis.** *Yonsei Med J* 1964;5:55–61 [CrossRef Medline](#)
- Oh SJ. **Spinal paragonimiasis.** *J Neurol Sci* 1968;6:125–40 [CrossRef Medline](#)
- Oh SJ. **Cerebral and spinal paragonimiasis: a histopathological study.** *J Neurol Sci* 1969;9:205–36 [CrossRef Medline](#)
- Qin Y, Cai J. **MRI findings of intraspinal extradural paragonimiasis granuloma in a child.** *Pediatr Radiol* 2012;42:1250–03 [CrossRef Medline](#)
- Gupta RK, Gupta S, Kumar S, et al. **MRI in intraspinal tuberculosis.** *Neuroradiology* 1994;36:39–43 [CrossRef Medline](#)
- Kumar S, Jain AK, Dhammi IK, et al. **Treatment of intraspinal tuberculoma.** *Clin Orthop Relat Res* 2007;460:62–66 [CrossRef Medline](#)
- Lee CH, Kim JH, Moon WS, et al. **Paragonimiasis in the abdominal cavity and subcutaneous tissue: report of 3 cases.** *Korean J Parasitol* 2012;50:345–47 [CrossRef Medline](#)
- Park CW, Chung WJ, Kwon YL, et al. **Consecutive extrapulmonary paragonimiasis involving liver and colon.** *J Dig Dis* 2012;13:186–89 [CrossRef Medline](#)
- Scharhoff T. **Paragonimiasis of the lung** [in German]. *Z Erkr Atmungsorgane* 1987;168:265–72 [Medline](#)
- Choi DW. **Paragonimus and paragonimiasis in Korea.** *Kisaengchunghak Chapchi* 1990;28(Suppl):79–102 [Medline](#)
- Yokogawa M. **Paragonimus and paragonimiasis.** *Adv Parasitol* 1965;3:99–158 [CrossRef Medline](#)

16. Peng X, Zhang J, Zhang J, et al. **Incidence of paragonimiasis in Chongqing China: a 6-year retrospective case review.** *Parasitology* 2018;145:792–96 [CrossRef Medline](#)
17. Diaz JH. **Paragonimiasis acquired in the United States: native and nonnative species.** *Clin Microbiol Rev* 2013;26:493–504 [CrossRef Medline](#)
18. Diaconita G, Nagy P. **Contributions to the study of intrarachidian localisation of distoma (paragonimiasis).** *Acta Med Scand* 1957; 159:151–54 [Medline](#)
19. Xia Y, Ju Y, Chen J, et al. **Hemorrhagic stroke and cerebral paragonimiasis.** *Stroke* 2014;45:3420–42 [CrossRef Medline](#)
20. Zhang JS, Huan Y, Sun LJ, et al. **MRI features of pediatric cerebral paragonimiasis in the active stage.** *J Magn Reson Imaging* 2006; 23:569–73 [CrossRef Medline](#)
21. Chang KH, Han MH. **MRI of CNS parasitic diseases.** *J Magn Reson Imaging* 1998;8:297–307 [CrossRef Medline](#)
22. Nomura M, Nitta H, Nakada M, et al. **MRI findings of cerebral paragonimiasis in chronic stage.** *Clin Radiol* 1999;54:622–64 [CrossRef Medline](#)
23. Cho SY, Hong ST, Rho YH, et al. **Application of micro-ELISA in serodiagnosis of human paragonimiasis.** *Kisaengchunghak Chapchi* 1981;19:151–56 [Medline](#)
24. Ozawa H, Kokubun S, Aizawa T, et al. **Spinal dumbbell tumors: an analysis of a series of 118 cases.** *J Neurosurg Spine* 2007;7:587–93 [CrossRef Medline](#)
25. Hetland S, Berg-Johnsen J, Heier T, et al. **Intraspinal hematoma after thoracic epidural analgesia** [in Norwegian]. *Tidsskr Nor Laegeforen* 1998;118:241–44 [Medline](#)
26. Colosimo C, Moschini M, Fileni A, et al. **Diagnostic imaging of intracranial and spinal lymphomas.** *Rays* 1994;19:490–510 [Medline](#)
27. Sakaida H, Waga S, Kojima T, et al. **Thoracic spinal angiomyolipoma with extracanal extension to the thoracic cavity: a case report.** *Spine (Phila Pa 1976)* 1998;23:391–94 [CrossRef Medline](#)